



M. Roghani · H. Rouhi

# Nonlinear stress-driven nonlocal formulation of Timoshenko beams made of FGMs

Received: 5 January 2020 / Accepted: 27 July 2020 / Published online: 5 August 2020  
© Springer-Verlag GmbH Germany, part of Springer Nature 2020

**Abstract** Motivated by the paradoxical results obtained from the differential nonlocal elasticity theory in some cases (e.g., bending and vibration problems of cantilevers), several attempts have been recently made to develop nonlocal beam models based on the integral (original) formulation of Eringen's nonlocal theory. These models can be classified into two main groups including strain- and stress-driven ones which have the capability of capturing the softening and hardening behaviors of material caused by nanoscale (nonlocal) effects, respectively. In the present paper, a novel stress-driven nonlocal formulation is developed for the nonlinear analysis of Timoshenko beams made of functionally graded materials. To this end, the governing equations are first derived in the context of integral form of stress-driven nonlocal model. The proposed model can be used for arbitrary kernel functions, and the paradox related to cantilever is resolved by it. The governing equations of stress-driven model in differential form together with corresponding constitutive boundary conditions are also derived. The Timoshenko beam under various end conditions is considered as the problem under study whose nonlinear static bending is analyzed. Furthermore, the generalized differential quadrature method is employed in the solution procedure. The effects of nonlocal parameter, FG index, length-to-thickness ratio and nonlinearity on the deflection of fully clamped, fully simply supported, clamped–simply supported and clamped–free beams are investigated. The presented formulation and results may be helpful in understanding nonlocal phenomena in nano-electro-mechanical systems.

**Keywords** Stress-driven nonlocal model · Timoshenko beam · Nonlinear bending · Paradox · Generalized differential quadrature

## 1 Introduction

The classical continuum theory is not appropriate for the mechanical analysis of micro- and nano-structures since it is scale-free and lacks length scale parameters. On the other hand, size-dependent elasticity theories such as the surface stress theory [1,2], strain gradient theories [3–6] and the nonlocal theory [7,8] are extensively employed to study the mechanical behaviors of materials at micro- and nano-scale owing to their capability to consider size influences. Among them, the nonlocal theory developed by Eringen and his co-workers [7–16] is a well-known non-classical elasticity theory in which behavior at a material point is affected by the state of

---

Communicated by Andreas Öchsner.

M. Roghani  
Faculty of Mechanical Engineering, University of Guilan, P.O. Box 3756, Rasht, Iran

H. Rouhi (✉)  
Department of Engineering Science, Faculty of Technology and Engineering, East of Guilan, University of Guilan, Rudsar-Vajargah 44891-63157, Iran  
E-mail: h\_rouhi@guilan.ac.ir

all points in the body. Using attenuation functions including the length scale parameter, the integral nonlocal constitutive equation, which considers multi-atom interactions, states that the stress at a reference point is a functional of the macroscopic Cauchy stress field at all point of the body. The general constitutive equations of nonlocal elasticity are expressed as [16]

$$t_{ij}(x) = \lambda \delta_{ij} \varepsilon_{kk}(x) + 2\mu \varepsilon_{ij}(x) \quad (1)$$

$$\sigma_{ij}(x') = \int_{\Omega} k(|x - x'|, l_c) t_{ij}(x) dx \quad (2)$$

where  $t_{ij}$  and  $\varepsilon_{ij}$  are the classical/local stress tensor and strain tensor, respectively;  $x'$ ,  $x$  indicate points of the continuum domain  $\Omega$ ;  $k$  is the attenuation or kernel function (nonlocal modulus);  $l_c$  is the nonlocal parameter; and  $|x - x'|$  denotes neighborhood distance. Also,  $\lambda$  and  $\mu$  denote Lamé's constants.

The integral nonlocal constitutive equation is formulated as a first kind Fredholm equation. In 1983, Eringen [17] showed that this integral equation can be transformed into the following differential equation for a specific class of attenuation functions (Green's function of linear differential operator)

$$(1 - l_c^2 \nabla^2) \sigma_{ij} = \lambda \delta_{ij} \varepsilon_{kk} + 2\mu \varepsilon_{ij} \quad (3)$$

in which  $l_c^2 = (e_0 a)^2$ , and  $\nabla^2$  is the Laplace operator.

Since working with this differential nonlocal constitutive equation is much easier than its integral counterpart, many researchers have applied it to study various mechanical behaviors of beam-, plate- and shell-type nano-structures up to now [18–25]. It was revealed that the nonlocal model in differential form can predict the results of molecular dynamics (MD) simulation on condition that its nonlocal parameter is correctly adjusted [26–29]. However, using the differential form of Eringen's theory may lead to some paradoxes. The first paradox was reported by Peddieson et al. [18]. They used the differential nonlocal constitutive equation in the context of Euler–Bernoulli (EB) beam theory to examine the behavior of cantilever microactuators. It was revealed that the nonlocal effect cannot be captured when the cantilever is under a concentrated load applied to its free end. Another important paradox happens in the case of the vibration problem of the nonlocal cantilever. Surprisingly, the first natural frequencies of clamped–free beam obtained by the differential nonlocal model are larger than those calculated based on the classical elasticity theory, whereas the nonlocality has a softening effect on the vibration of beams with other types of end conditions [20, 30, 31]. A similar paradox exists in the bending problem of nonlocal cantilever (hardening behavior instead of softening behavior with increasing the nonlocal parameter) [32, 33]. For experimental results on this problem, the reader is referred to the paper of Abazari et al. [34] in which size effects on the mechanical properties of micro- and nano-structures were studied. In that paper, they summarized experimental data for the size effect on the effective Young's modulus ( $E_{\text{eff}}$ ) of beams under clamped–free and clamped–clamped boundary conditions made of various materials with different morphologies. It was reported that in most cases,  $E_{\text{eff}}$  increases when size reduces. Challamel et al. [35] explained that these paradoxical behaviors are due to nonself-adjointness property of the energy functional of nonlocal differential model which can be related to a non-conservative inertia moment acting on the beam free end. This indicates that the differential model results in non-conservative problems. They constructed a functional by an inverse procedure in which the end conditions were amended to make the problem self-adjoint. Also, several researchers resolved the mentioned paradoxes using the integral nonlocal constitutive equation. The reader is referred to the papers of Khodabakhshi and Reddy [36], Fernández-Sáez et al. [37], Zhu and Li [38], Norouzzadeh et al. [39, 40], Tuna and Kirca [41] and Koutsoumaris et al. [42] as some examples.

Recently, Romano et al. [43–47] formulated and applied the integral nonlocal theory in an unconventional way. In their integral nonlocal model, which is called “stressdriven,” the roles of stress and strain fields are swapped. The constitutive relations of this model are given by

$$\sigma_{ij}(x') = \lambda \delta_{ij} \varepsilon_{kk}(x') + 2\mu \varepsilon_{ij}(x') \quad (4)$$

$$\sigma_{ij}(x') = \int_{\Omega} k(|x - x'|, l_c) t_{ij}(x) dx \quad (5)$$

where  $\sigma_{ij}$  is the local stress tensor and  $t_{ij}$  is the nonlocal stress tensor.

The motivation for developing the “stressdriven” model versus its counterpart, i.e., the “straindriven” model, can be explained as follows. According to the strain-driven model, the elastic strain is introduced via a Fredholm-type integral equation in which the stress is the production of a convolution between the local response to an

elastic strain and the attenuation function. The strain-driven nonlocal integral model has been employed by numerous research workers based on a differential formulation equivalent to the integral formulation (e.g., [37]). Romano et al. [46] commented that this equivalence must be supplemented by satisfying constitutive boundary conditions. Furthermore, because of incompatibility between nonlocal stress–strain equations and equilibrium condition, the problem derived based on the strain-driven model can be ill-posed [46]. It has been revealed that the stress-driven model has not the stated conflict of strain-driven model and results in a well-posed problem in general case.

After Romano et al., some attempts have been made at developing nonlocal formulations based on the stress-driven model (e.g., [48–51]). For example, Faraji Oskouie et al. [49–51] published some papers on the mechanical behaviors of small-scale structures based upon the strain- and stress-driven nonlocal models. In [49], in the context of integral formulation of nonlocal elasticity, a numerical strategy was proposed to investigate the linear bending of EB beams based upon strain- and stress-driven models. It was shown that paradoxical results associated with the static bending of nanocantilever can be resolved using the integral stress-driven model. Also, in [50], the strain- and stress-driven nonlocal models were used to study the free vibration and buckling of EB beams under arbitrary end supports. In another work [51], three size-dependent formulations were proposed for the linear analysis of beams based on the integral nonlocal and strain gradient theories. According to the stress-driven nonlocal and strain gradient models, the bending and free vibration of Timoshenko nanobeams were numerically studied. In addition, Faraji Oskouie et al. [52] addressed the linear bending problem of Timoshenko beams by combining the nonlocal and micropolar theories.

In the current work, on the basis of integral formulation of nonlocal theory, a novel nonlinear stress-driven nonlocal formulation is proposed for the Timoshenko beams made of FGMs. The developed formulation is applicable for arbitrary kernel functions. Moreover, it is capable of resolving the paradox related to clamped–free boundary conditions. The focus of the paper is on the geometrically nonlinear static bending. The GDQ method is also utilized in the solution approach. The influences of nonlocal parameter, end conditions and FG index on the large deformation response of the beams are studied. Moreover, comparisons are provided between the results of linear and nonlinear models.

## 2 FG Timoshenko beam model

The displacement field in a Timoshenko beam can be written as

$$u_x = u + z\psi, \quad u_y = 0, \quad u_z = w \quad (6)$$

where  $u_x$ ,  $u_y$  and  $u_z$  are displacement components along the length ( $x$ ), width ( $y$ ) and thickness ( $z$ ) directions, respectively. Figure 1 indicates the coordinate system and geometrical properties. Furthermore,  $u$  and  $w$  show the axial and transverse displacements on the physical middle surface, respectively. Considering the von-Kármán geometric nonlinearity, the strain components are given by

$$\epsilon_{xx} = \frac{\partial u}{\partial x} + \frac{1}{2} \left( \frac{\partial w}{\partial x} \right)^2 + z \frac{\partial \psi}{\partial x} \equiv \epsilon_{xx}^0 + z\epsilon_{xx}^1, \quad \gamma_{xz} = \left( \frac{\partial w}{\partial x} + \psi \right) \equiv \gamma_{xz}^0. \quad (7)$$

Note that the nonlinearity owing to the stretching influence of mid-plane of the FG beam is considered in the strain component  $\epsilon_{xx}$ . Constitutive relations are given as

$$\sigma_{xx} = E(z)\epsilon_{xx}, \quad \sigma_{xz} = k_s G(z) \gamma_{xz} \quad (8)$$

in which  $E(z)$  and  $G(z)$  denote elastic and shear moduli, respectively. Moreover,  $k_s$  indicates the shear correction factor. Combining Eqs. (7) and (8) leads to

$$\sigma_{xx} = E(z) \left( \frac{\partial u}{\partial x} + \frac{1}{2} \left( \frac{\partial w}{\partial x} \right)^2 + z \frac{\partial \psi}{\partial x} \right), \quad \sigma_{xz} = k_s G(z) \left( \frac{\partial w}{\partial x} + \psi \right). \quad (9)$$

Also, the FGM properties are calculated as follows

$$P(z) = (P_m - P_c) \left( \frac{z}{h} + \frac{1}{2} \right)^n + P_c \quad (10)$$

where  $P(z)$  denotes the material property along the  $z$  direction. Moreover,  $m$  and  $c$  subscripts stand for metal and ceramic phases, respectively.

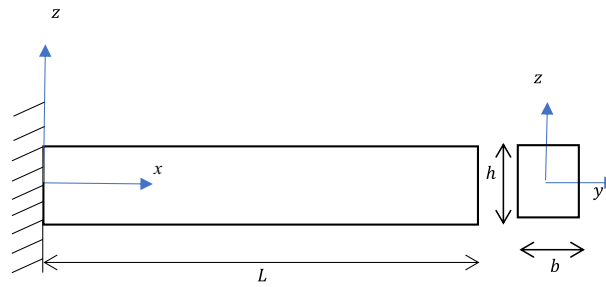


**Fig. 1** Coordinate system and geometrical parameters

### 3 Governing equations

In the context of the stress-driven nonlocal model, the stress–strain equations are expressed as follows

$$\sigma_{ij} = \lambda \delta_{ij} \epsilon_{kk} + 2\mu \epsilon_{ij} \quad (11)$$

$$\sigma_{ij} = \int_{\Omega} k(|x - x'|, l_c) t_{ij} dx \quad (12)$$

where  $k$  and  $l_c$  are the kernel function and nonlocal parameter, respectively. The kernel in one-dimensional case can be expressed as

$$\alpha\{|x - x'|, l_c\} = \frac{1}{2l_c} e^{-\frac{|x-x'|}{l_c}}, \quad l_c = e_0 a. \quad (13)$$

Using Eqs. (6) and (7), the stress-driven nonlocal constitutive equations are derived as

$$E(z) \epsilon_{xx} = E(z) \left( \frac{\partial u}{\partial x} + \frac{1}{2} \left( \frac{\partial w}{\partial x} \right)^2 + z \frac{\partial \psi}{\partial x} \right) = \int_x \frac{1}{2l_c} e^{-\frac{|x-x'|}{l_c}} t_{xx} dx \quad (14)$$

$$k_s G(z) \epsilon_{xz} = k_s G(z) \left( \frac{\partial w}{\partial x} + \psi \right) = \int_x \frac{1}{2l_c} e^{-\frac{|x-x'|}{l_c}} t_{xz} dx. \quad (15)$$

Accordingly, the resultant bending moment and shear force are obtained as

$$B_{11} \left( \frac{\partial u}{\partial x} + \frac{1}{2} \left( \frac{\partial w}{\partial x} \right)^2 \right) + D_{11} \left( \frac{\partial \psi}{\partial x} \right) = \int_0^L \frac{1}{2l_c} e^{-\frac{|x-x'|}{l_c}} M_{xx} dx \quad (16)$$

$$A_{11} \left( \frac{\partial u}{\partial x} + \frac{1}{2} \left( \frac{\partial w}{\partial x} \right)^2 \right) + B_{11} \left( \frac{\partial \psi}{\partial x} \right) = \int_0^L \frac{1}{2l_c} e^{-\frac{|x-x'|}{l_c}} N_{xx} dx \quad (17)$$

$$A_{55} \left( \frac{\partial w}{\partial x} + \psi \right) = \int_0^L \frac{1}{2l_c} e^{-\frac{|x-x'|}{l_c}} Q_x dx. \quad (18)$$

The terms related to stiffness components in Eqs. (16)–(18) can be defined as

$$\{A_{11}, B_{11}, D_{11}\} = \int_{-\frac{h}{2}}^{\frac{h}{2}} \int_{-\frac{b}{2}}^{\frac{b}{2}} E(z) \{1, (z - z_0), (z - z_0)^2\} dy dz \quad (19)$$

$$A_{55} = \frac{k_s}{2(1 + \nu)} \int_{-\frac{h}{2}}^{\frac{h}{2}} \int_{-\frac{b}{2}}^{\frac{b}{2}} E(z) dy dz \quad (20)$$

where  $z_0$  denotes the position of the neutral axis of the beam given by [53]

$$z_0 = \left( \int_{-\frac{h}{2}}^{\frac{h}{2}} z E(z) dz \right) / \left( \int_{-\frac{h}{2}}^{\frac{h}{2}} E(z) dz \right). \quad (21)$$

The integral form of Eqs. (16)–(18) is converted to the differential form here. For this aim, one can write

$$M_{xx} = B_{11} \left( 1 - l_c^2 \frac{\partial^2}{\partial x^2} \right) \left( \frac{\partial u}{\partial x} + \frac{1}{2} \left( \frac{\partial w}{\partial x} \right)^2 \right) + D_{11} \left( 1 - l_c^2 \frac{\partial^2}{\partial x^2} \right) \frac{\partial \psi}{\partial x} \quad (22)$$

$$N_{xx} = A_{11} \left( 1 - l_c^2 \frac{\partial^2}{\partial x^2} \right) \left( \frac{\partial u}{\partial x} + \frac{1}{2} \left( \frac{\partial w}{\partial x} \right)^2 \right) + B_{11} \left( 1 - l_c^2 \frac{\partial^2}{\partial x^2} \right) \frac{\partial \psi}{\partial x} \quad (23)$$

$$Q_x = A_{55} \left( 1 - l_c^2 \frac{\partial^2}{\partial x^2} \right) \left( \frac{\partial w}{\partial x} + \psi \right). \quad (24)$$

This procedure leads to a series of constitutive boundary conditions which should also be satisfied. Constitutive boundary conditions associated with the stress-driven integral model for Timoshenko beams, governed by Helmholtz averaging kernel, were established in [54]. Constitutive boundary conditions for the present problem are expressed as

$$\left( \frac{\partial^2 \psi}{\partial x^2} - \frac{1}{l_c} \frac{\partial \psi}{\partial x} \right) \Big|_{x=0} = 0 \quad (25)$$

$$\left( \frac{\partial^2 \psi}{\partial x^2} + \frac{1}{l_c} \frac{\partial \psi}{\partial x} \right) \Big|_{x=L} = 0 \quad (26)$$

$$\left( \frac{\partial^2 w}{\partial x^2} + \frac{\partial \psi}{\partial x} - \frac{1}{l_c} \left( \frac{\partial w}{\partial x} + \psi \right) \right) \Big|_{x=0} = 0 \quad (27)$$

$$\left( \frac{\partial^2 w}{\partial x^2} + \frac{\partial \psi}{\partial x} + \frac{1}{l_c} \left( \frac{\partial w}{\partial x} + \psi \right) \right) \Big|_{x=L} = 0. \quad (28)$$

Furthermore, the principle of virtual displacement for the Timoshenko beam is [55]

$$\int_0^L (N_{xx} \delta \epsilon_{xx}^0 + M_{xx} \delta \epsilon_{xx}^1 + Q_x \delta \gamma_{xz}^0 - q \delta w) dx = 0. \quad (29)$$

From above equation, one can arrive at the following Euler–Lagrange equations

$$\delta w: \frac{\partial Q_x}{\partial x} + \frac{\partial}{\partial x} \left( N_{xx} \frac{\partial w}{\partial x} \right) + q = 0 \quad (30)$$

$$\delta \psi: \frac{\partial M_{xx}}{\partial x} - Q_x = 0 \quad (31)$$

$$\delta u: \frac{\partial N_{xx}}{\partial x} = 0. \quad (32)$$

The corresponding boundary conditions are also given by

$$N_{xx}|_{x=0,L} = 0, \quad \text{or} \quad \delta u|_{x=0,L} = 0 \quad (33)$$

$$M_{xx}|_{x=0,L} = 0, \quad \text{or} \quad \delta \psi|_{x=0,L} = 0 \quad (34)$$

$$\left[ Q_{xz} + N_{xx} \frac{\partial w}{\partial x} \right] \Big|_{x=0,L} = 0, \quad \text{or} \quad \delta w|_{x=0,L} = 0. \quad (35)$$

By inserting the resultants of Eqs. (22)–(24) into Eqs. (30)–(32), the differential form of governing equations is derived as

$$\begin{aligned} & \frac{\partial}{\partial x} \left[ A_{55} \left( 1 - l_c^2 \frac{\partial^2}{\partial x^2} \right) \left( \frac{\partial w}{\partial x} + \psi \right) \right] \\ & + \frac{\partial}{\partial x} \left[ A_{11} \frac{\partial w}{\partial x} \left( 1 - l_c^2 \frac{\partial^2}{\partial x^2} \right) \left( \frac{\partial u}{\partial x} + \frac{1}{2} \left( \frac{\partial w}{\partial x} \right)^2 \right) + B_{11} \frac{\partial w}{\partial x} \left( 1 - l_c^2 \frac{\partial^2}{\partial x^2} \right) \frac{\partial \psi}{\partial x} \right] + q = 0 \end{aligned} \quad (36)$$

$$\begin{aligned} \frac{\partial}{\partial x} \left[ B_{11} \left( 1 - l_c^2 \frac{\partial^2}{\partial x^2} \right) \left( \frac{\partial u}{\partial x} + \frac{1}{2} \left( \frac{\partial w}{\partial x} \right)^2 \right) + D_{11} \left( 1 - l_c^2 \frac{\partial^2}{\partial x^2} \right) \frac{\partial \psi}{\partial x} \right] \\ - A_{55} \left( 1 - l_c^2 \frac{\partial^2}{\partial x^2} \right) \left( \frac{\partial w}{\partial x} + \psi \right) = 0 \end{aligned} \tag{37}$$

$$\frac{\partial}{\partial x} \left[ A_{11} \left( 1 - l_c^2 \frac{\partial^2}{\partial x^2} \right) \left( \frac{\partial u}{\partial x} + \frac{1}{2} \left( \frac{\partial w}{\partial x} \right)^2 \right) + B_{11} \left( 1 - l_c^2 \frac{\partial^2}{\partial x^2} \right) \frac{\partial \psi}{\partial x} \right] = 0 \tag{38}$$

Finally, a system of coupled equations together with corresponding boundary conditions is obtained. Using the following non-dimensional parameters

$$\begin{aligned} \bar{A}_{11} &= \frac{A_{11}}{A_{11}^0}, & \bar{B}_{11} &= \frac{B_{11}}{A_{11}^0 h}, & \bar{D}_{11} &= \frac{D_{11}}{A_{11}^0 h^2}, & \bar{A}_{55} &= \frac{A_{55}}{A_{11}^0} \\ \bar{x} &= \frac{x}{L}, & \bar{w} &= \frac{w}{h}, & \bar{u} &= \frac{u}{h}, & \bar{\psi} &= \psi, & \bar{q} &= \frac{qL^2}{hA_{11}^0} \\ \lambda &= \frac{l_c}{L}, & \eta &= \frac{h}{L}, \end{aligned} \tag{39}$$

the governing equations (36)–(38) can be re-written as

$$\begin{aligned} \frac{\partial}{\partial \bar{x}} \left[ \bar{A}_{55} \left( 1 - \lambda^2 \frac{\partial^2}{\partial \bar{x}^2} \right) \left( \frac{\partial \bar{w}}{\partial \bar{x}} + \frac{\bar{\psi}}{\eta} \right) \right] \\ + \frac{\partial}{\partial \bar{x}} \left[ \bar{A}_{11} \eta \frac{\partial \bar{w}}{\partial \bar{x}} \left( 1 - \lambda^2 \frac{\partial^2}{\partial \bar{x}^2} \right) \left( \frac{\partial \bar{u}}{\partial \bar{x}} + \frac{1}{2} \eta \left( \frac{\partial \bar{w}}{\partial \bar{x}} \right)^2 \right) + \bar{B}_{11} \eta \frac{\partial \bar{w}}{\partial \bar{x}} \left( 1 - \lambda^2 \frac{\partial^2}{\partial \bar{x}^2} \right) \frac{\partial \bar{\psi}}{\partial \bar{x}} \right] + \bar{q} = 0 \end{aligned} \tag{40}$$

$$\begin{aligned} \frac{\partial}{\partial \bar{x}} \left[ \bar{B}_{11} \eta \left( 1 - \lambda^2 \frac{\partial^2}{\partial \bar{x}^2} \right) \left( \frac{\partial \bar{u}}{\partial \bar{x}} + \frac{1}{2} \eta \left( \frac{\partial \bar{w}}{\partial \bar{x}} \right)^2 \right) + \bar{D}_{11} \eta \left( 1 - \lambda^2 \frac{\partial^2}{\partial \bar{x}^2} \right) \frac{\partial \bar{\psi}}{\partial \bar{x}} \right] \\ - \bar{A}_{55} \left( 1 - \lambda^2 \frac{\partial^2}{\partial \bar{x}^2} \right) \left( \frac{\partial \bar{w}}{\partial \bar{x}} + \frac{\bar{\psi}}{\eta} \right) = 0 \end{aligned} \tag{41}$$

$$\frac{\partial}{\partial \bar{x}} \left[ \bar{A}_{11} \left( 1 - \lambda^2 \frac{\partial^2}{\partial \bar{x}^2} \right) \left( \frac{\partial \bar{u}}{\partial \bar{x}} + \frac{1}{2} \eta \left( \frac{\partial \bar{w}}{\partial \bar{x}} \right)^2 \right) + \bar{B}_{11} \left( 1 - \lambda^2 \frac{\partial^2}{\partial \bar{x}^2} \right) \frac{\partial \bar{\psi}}{\partial \bar{x}} \right] = 0. \tag{42}$$

### 4 Solution by GDQ

Based on the idea of the GDQ method, the  $r$ th-order derivative of function  $f(x)$  at a given point  $x_i$  on the domain  $[x_1, \dots, x_N]$  is approximated as

$$\frac{d^r f(x)}{dx^r} = \sum_{j=1}^N D_{ij}^{(r)} f(x_j) \tag{43}$$

where  $D_{ij}^{(r)}$  shows the weighting coefficients of  $r$ th-order derivative which can be calculated by

$$\left[ D_x^{(r)} \right] = W_{ij}^{(r)} = \begin{cases} I_{ij}, & \text{where } I_{ij} \text{ is a } N \times N \text{ identity matrix } r = 0 \\ \frac{P(x_i)}{(x_i - x_j)P(x_j)}, & \text{where } P(x_i) = \prod_{k=1; i \neq k}^N (x_i - x_k) \\ & i, j = 1, \dots, N \text{ and } i \neq j \text{ and } r = 1 \\ \left\{ \begin{aligned} r \left[ W_{ij}^{(1)} W_{ii}^{(r-1)} - \frac{W_{ij}^{(r-1)}}{x_i - x_j} \right], & \text{and } i \neq j \\ - \sum_{\substack{k=1 \\ k \neq i}}^N W_{ik}^{(r-1)}, & \text{and } i = j \end{aligned} \right. & \\ i, j = 1, \dots, N & \text{and } r \geq 2 \end{cases} \tag{44}$$

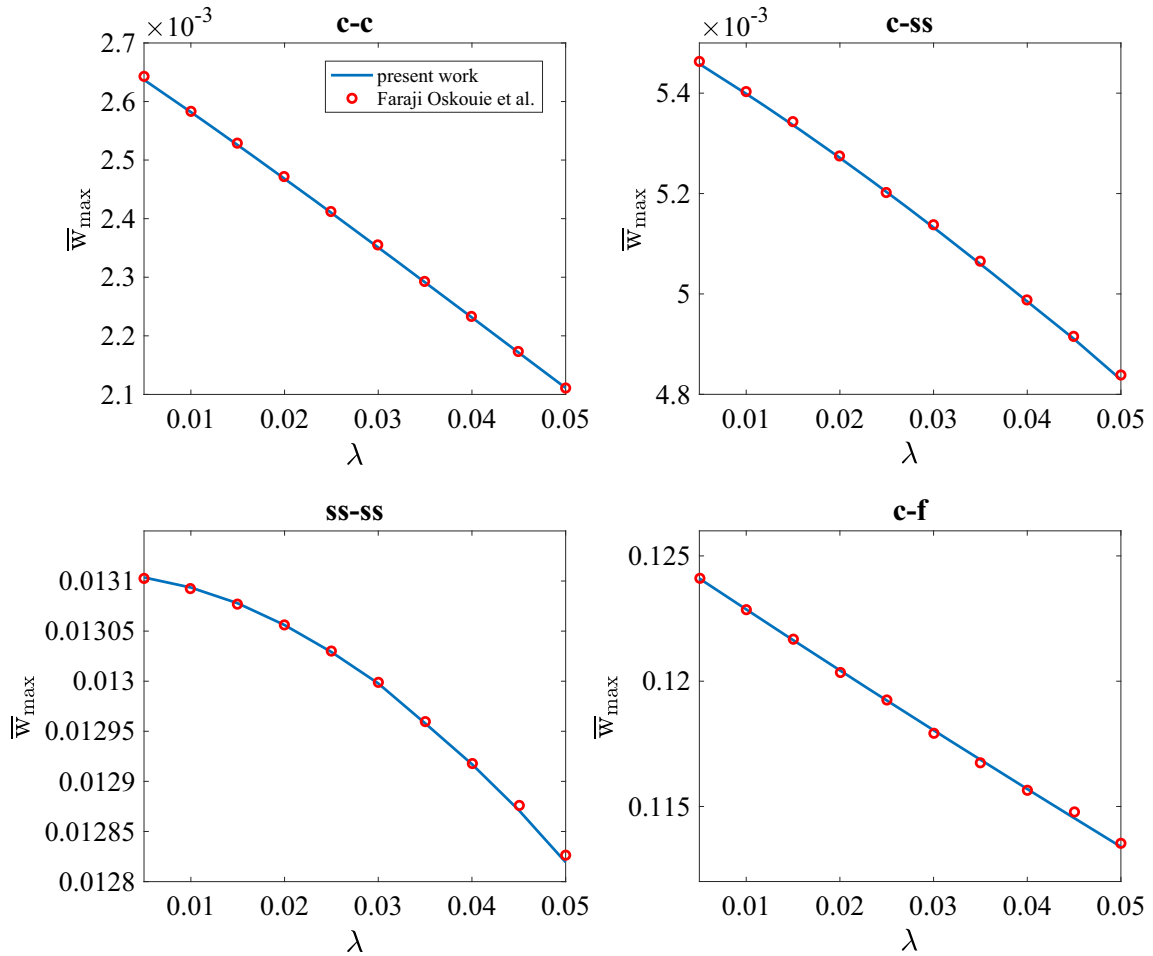


**Fig. 2** Variation of maximum non-dimensional deflection with  $\lambda$  for various boundary conditions ( $n = 0, L/h = 25$  and  $\bar{q} = 1$ )

With the shifted Chebyshev–Gauss–Lobatto grid distribution, the grid points in the  $x$ - and  $y$ -directions can be selected as

$$x_i = \frac{1}{2} \left( 1 - \cos \left( \frac{i-1}{N-1} \pi \right) \right), \quad i = 1, 2, 3, \dots, N. \tag{45}$$

Finally, inserting the discretized forms of displacement field variables and their derivatives in the governing equations presented in Eqs. (40), (42) along with boundary conditions leads to the following equation

$$\mathbf{KX} + \mathbf{N}(\mathbf{X}) = \mathbf{F} \tag{46}$$

where  $\mathbf{X}$ ,  $\mathbf{K}$  and  $\mathbf{N}(\mathbf{X})$  represent the displacement vector, the stiffness matrix and the nonlinear part vector, which are given by

$$\mathbf{X} = [\bar{w}^T \ \bar{\psi}^T \ \bar{u}^T]^T \tag{47}$$

$$\mathbf{N}(\mathbf{X}) = [N_w^T(X), N_\psi^T(X), N_u^T(X)]^T \tag{48}$$

$$\mathbf{K} = \begin{bmatrix} K_{ww} & K_{w\psi} & K_{wu} \\ K_{\psi w} & K_{\psi\psi} & K_{\psi u} \\ K_{uw} & K_{u\psi} & K_{uu} \end{bmatrix}. \tag{49}$$

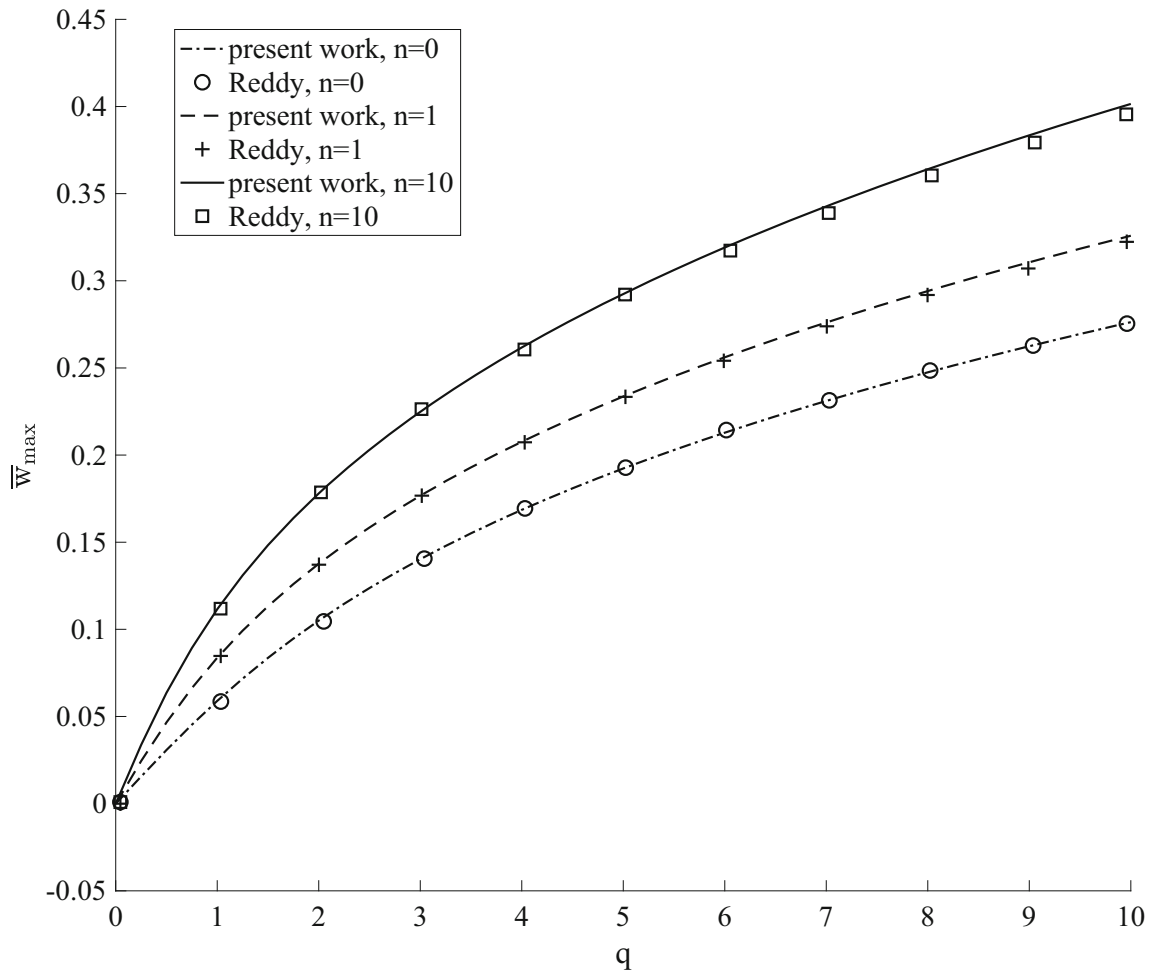


**Fig. 3** Variation of maximum non-dimensional deflection with load ( $q$ ) for C-SS boundary conditions and various FGM non-homogeneity indexes

The components of  $\mathbf{K}$  and  $\mathbf{N}(\mathbf{X})$  take the following form

$$K_{ww} = \bar{A}_{55} \left( \mathbf{D}_{\bar{x}}^{(0)} - \lambda^2 \mathbf{D}_{\bar{x}}^{(2)} \right) \mathbf{D}_{\bar{x}}^{(2)} \tag{50}$$

$$K_{w\psi} = \bar{A}_{55} \left( \mathbf{D}_{\bar{x}}^{(0)} - \lambda^2 \mathbf{D}_{\bar{x}}^{(2)} \right) \mathbf{D}_{\bar{x}}^{(1)} / \eta \tag{51}$$

$$K_{wu} = 0 \tag{52}$$

$$K_{\psi w} = -\bar{A}_{55} \left( \mathbf{D}_{\bar{x}}^{(0)} - \lambda^2 \mathbf{D}_{\bar{x}}^{(2)} \right) \mathbf{D}_{\bar{x}}^{(1)} \tag{53}$$

$$K_{\psi\psi} = -\bar{A}_{55} \left( \mathbf{D}_{\bar{x}}^{(0)} - \lambda^2 \mathbf{D}_{\bar{x}}^{(2)} \right) \mathbf{D}_{\bar{x}}^{(0)} / \eta + \bar{D}_{11} \eta \left( \mathbf{D}_{\bar{x}}^{(0)} - \lambda^2 \mathbf{D}_{\bar{x}}^{(2)} \right) \mathbf{D}_{\bar{x}}^{(2)} \tag{54}$$

$$K_{\psi u} = \bar{B}_{11} \eta \left( \mathbf{D}_{\bar{x}}^{(0)} - \lambda^2 \mathbf{D}_{\bar{x}}^{(2)} \right) \mathbf{D}_{\bar{x}}^{(2)} \tag{55}$$

$$K_{uw} = 0 \tag{56}$$

$$K_{u\psi} = \bar{B}_{11} \left( \mathbf{D}_{\bar{x}}^{(0)} - \lambda^2 \mathbf{D}_{\bar{x}}^{(2)} \right) \mathbf{D}_{\bar{x}}^{(2)} \tag{57}$$

$$K_{uu} = \bar{A}_{11} \left( \mathbf{D}_{\bar{x}}^{(0)} - \lambda^2 \mathbf{D}_{\bar{x}}^{(2)} \right) \mathbf{D}_{\bar{x}}^{(2)} \tag{58}$$

$$N_w^T(\mathbf{X}) = \mathbf{D}_{\bar{x}}^{(1)} \left[ \bar{A}_{11} \eta \left( \mathbf{D}_{\bar{x}}^{(1)} \bar{w} \right) \circ \left( \mathbf{D}_{\bar{x}}^{(0)} - \lambda^2 \mathbf{D}_{\bar{x}}^{(2)} \right) \left( \mathbf{D}_{\bar{x}}^{(1)} \bar{u} + \frac{1}{2} \eta \left( \mathbf{D}_{\bar{x}}^{(1)} \bar{w} \right)^2 \right) \right]$$



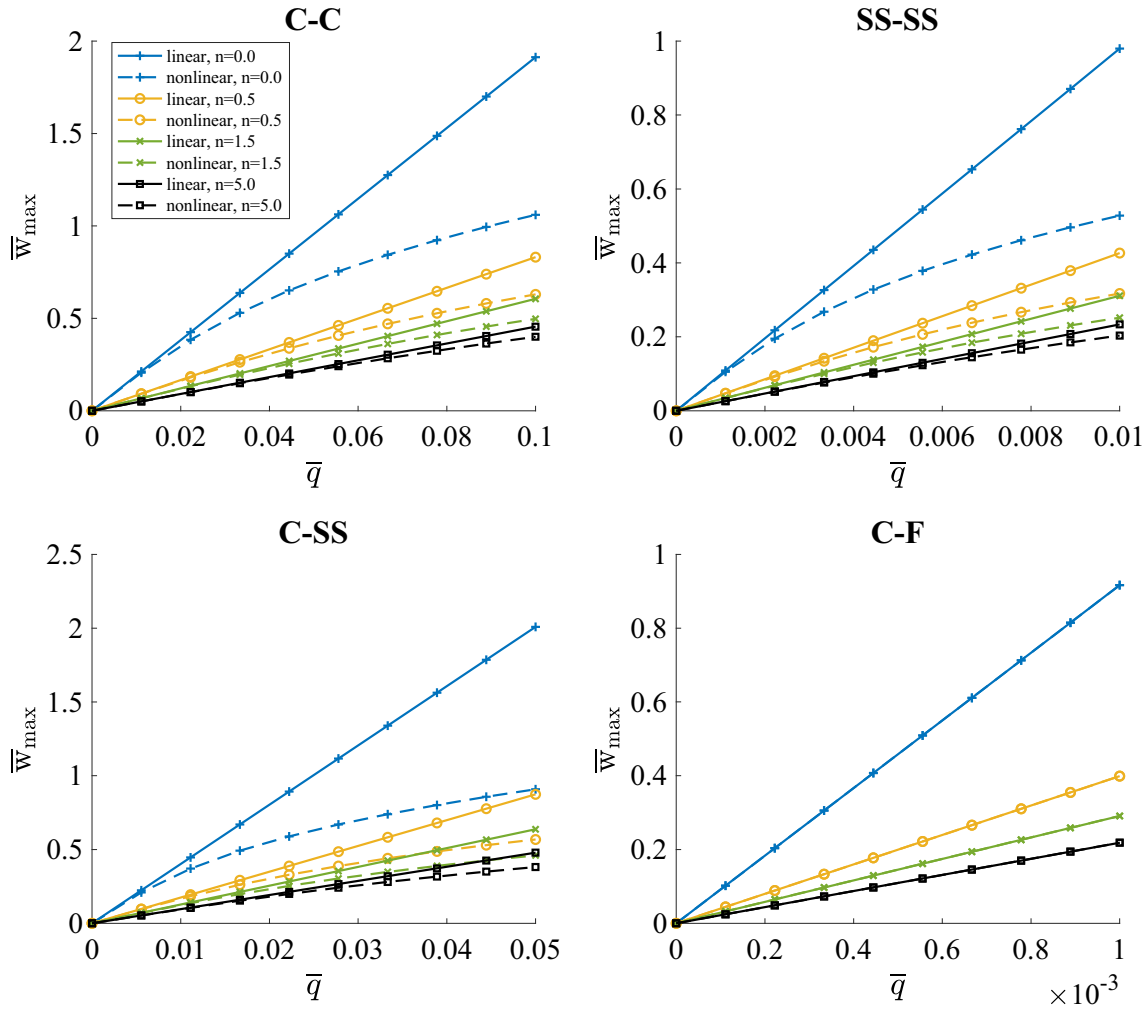


**Fig. 4** Variation of maximum non-dimensional deflection with dimensionless load ( $\bar{q}$ ) for various boundary conditions and FGM non-homogeneity indexes based on linear and nonlinear models ( $\lambda = 0.01$ )

$$+ \bar{B}_{11} \eta \left( \mathbf{D}_{\bar{x}}^{(1)} \bar{w} \right) \circ \left( \mathbf{D}_{\bar{x}}^{(0)} - \lambda^2 \mathbf{D}_{\bar{x}}^{(2)} \right) \left( \mathbf{D}_{\bar{x}}^{(1)} \bar{\psi} \right) \quad (59)$$

$$N_{\psi}^T(X) = \mathbf{D}_{\bar{x}}^{(1)} \left[ \bar{B}_{11} \eta \left( \mathbf{D}_{\bar{x}}^{(0)} - \lambda^2 \mathbf{D}_{\bar{x}}^{(2)} \right) \left( \frac{1}{2} \eta \left( \mathbf{D}_{\bar{x}}^{(1)} \bar{w} \right)^2 \right) \right] \quad (60)$$

$$N_u^T(X) = \mathbf{D}_{\bar{x}}^{(1)} \left[ \bar{A}_{11} \left( \mathbf{D}_{\bar{x}}^{(0)} - \lambda^2 \mathbf{D}_{\bar{x}}^{(2)} \right) \left( \frac{1}{2} \eta \left( \mathbf{D}_{\bar{x}}^{(1)} \bar{w} \right)^2 \right) \right] \quad (61)$$

In above equations,  $\circ$  shows the Hadamard product. The system of nonlinear equations presented as Eq. (46) is solved by the well-known Newton–Raphson method in order to obtain the displacement field.

## 5 Results

First, two comparison studies are presented to validate the developed formulation and numerical approach. In the first case, a comparison is provided between the present results and those reported in [51] for the linear bending of Timoshenko nanobeam based on the stress-driven integral nonlocal model. Figure 2 shows the variation of dimensionless maximum deflection of beams ( $\bar{w}_{\max}$ ) versus  $\lambda$  for various boundary conditions. It is observed that there is an excellent agreement between the current results and the ones given in [51].

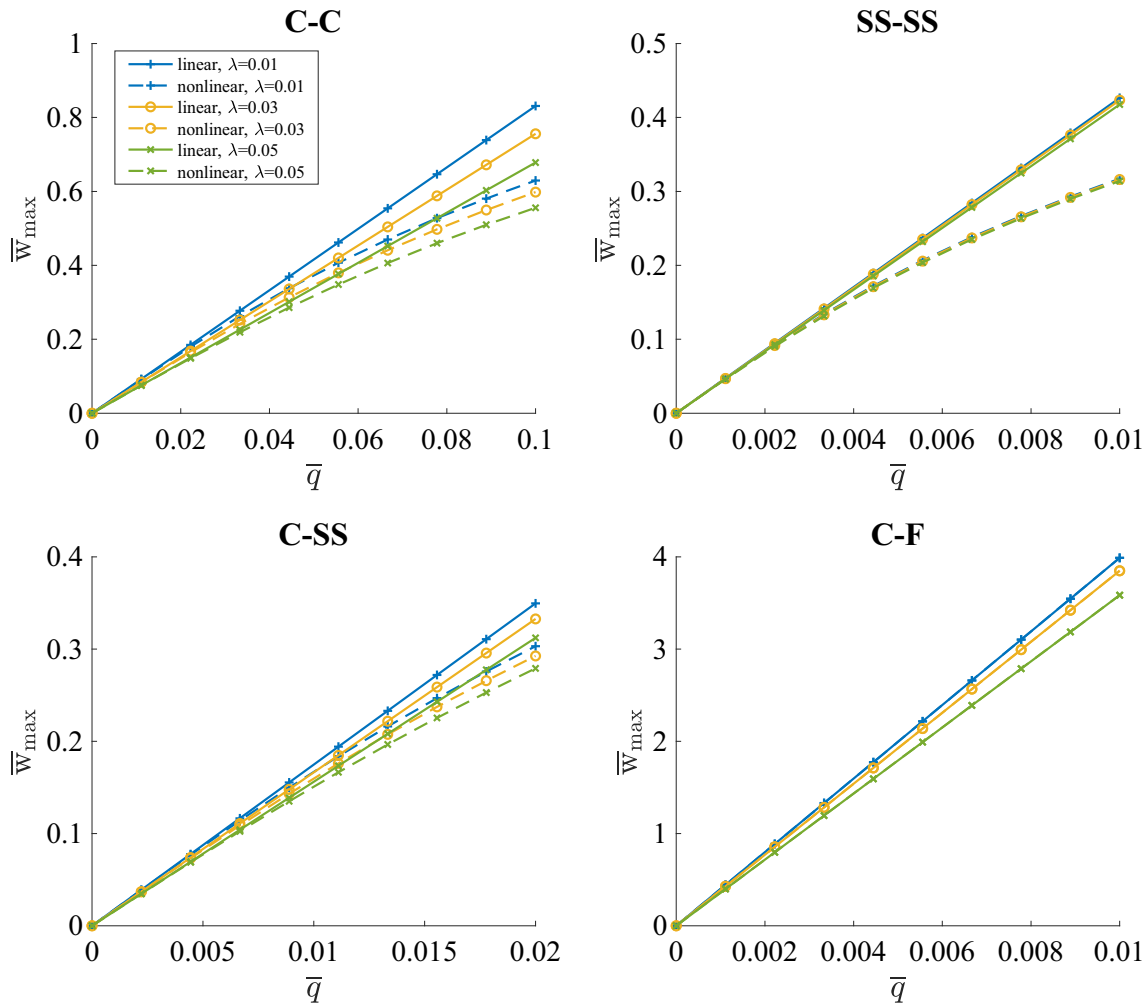


**Fig. 5** Variation of maximum non-dimensional deflection with dimensionless load ( $\bar{q}$ ) for various boundary conditions and values of  $\lambda$  based on linear and nonlinear models ( $n = 0.5$ )

Another validation study is presented for the nonlinear bending of classical Timoshenko beam with comparison to the results of [55] in Fig. 3. This figure indicates the variation of maximum non-dimensional deflection against load ( $q$ ) for FG beam under C–SS (clamped–simply supported) end conditions considering three values of FG index. Again, the validity of present work is assured.

For the rest of results, the material properties are taken as [51,53]

$$E_c = 393 \text{ GPa}, \quad E_m = 68.5 \text{ GPa}, \quad \nu = 0.35$$

Moreover, the length-to-thickness ratio is assumed as 25 considering  $b/h = 1$ , otherwise stated. In Figs. 4, 5 and 6, the dimensionless maximum deflection of nanobeams is plotted versus dimensionless load ( $\bar{q}$ ) for SS–SS (fully simply supported), C–C (fully clamped), C–F (cantilever) and C–SS end conditions. The results of these figures are generated based on both linear and nonlinear models. Figure 4 shows the effect of FG index on the nonlinear bending of Timoshenko nanobeams based on the stress-driven nonlocal model. One can find that at a given applied load, the deflection of beam decreases as the FG index gets larger. In Fig. 5, the effect of nonlocality can be investigated. The results of this figure are calculated considering three values of  $\lambda$  including 0.01, 0.03 and 0.05. It is observed that for all boundary conditions, increasing  $\lambda$  has a decreasing effect on the deflection of nanobeam. As Fig. 5 indicates, consistent results are obtained by the present approach in the case of nanocantilever. Finally, Fig. 6 highlights the influence of length-to-thickness ratio. As expected, decrease in the mentioned ratio leads to decreasing the maximum deflection.

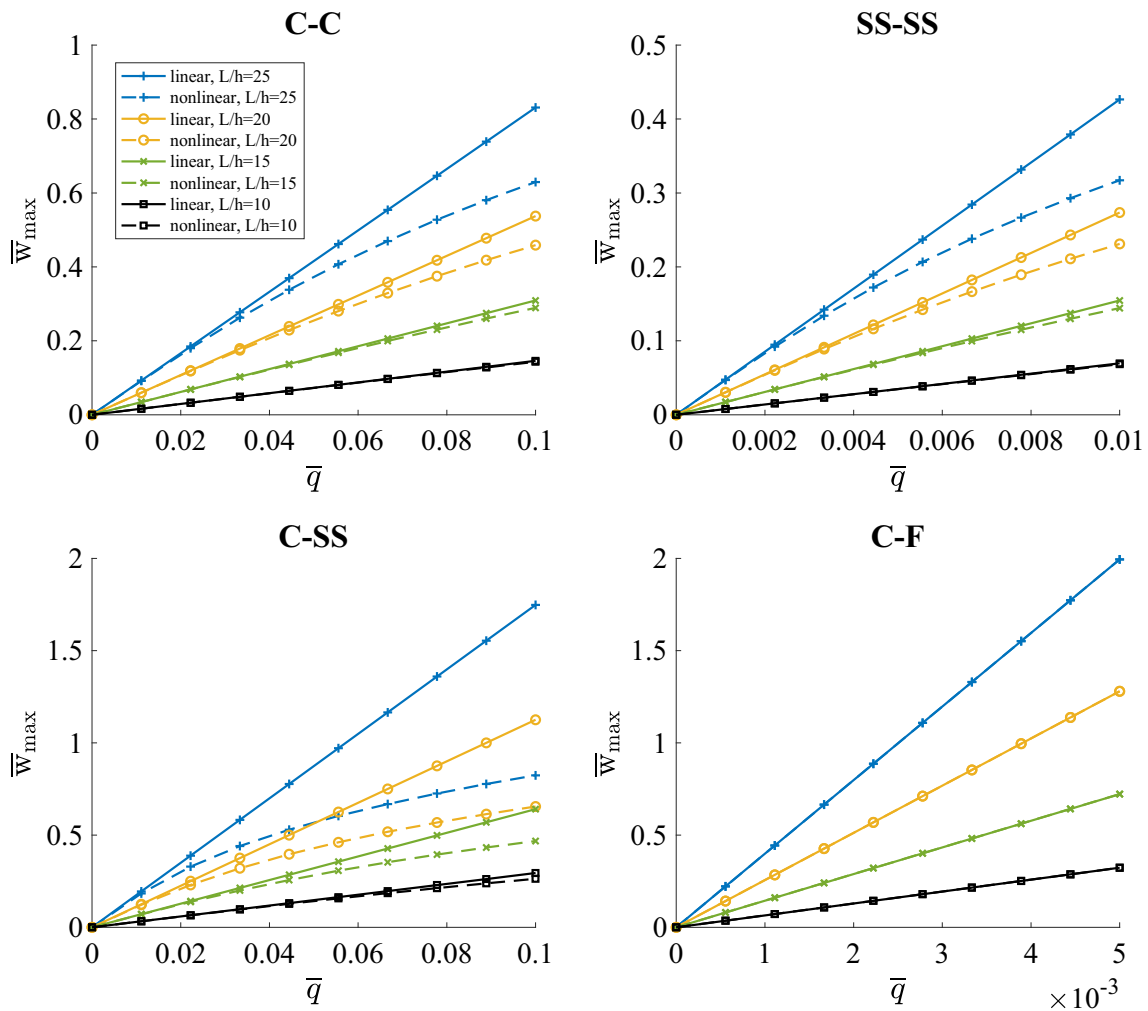


**Fig. 6** Variation of maximum non-dimensional deflection with dimensionless load ( $\bar{q}$ ) for various boundary conditions and values of  $L/h$  based on linear and nonlinear models ( $\lambda = 0.01, n = 0.5$ )

### 6 Conclusion

In the present article, within the framework of integral (original) form of Eringen’s nonlocal elasticity and based on the stress-driven model, a numerical approach was presented for the nonlinear analysis of beam-type small-scale structures. The beams were modeled according to the Timoshenko beam theory, and it was considered that they are made of FGMs. First, the governing equations were obtained based upon the integral form of stress-driven nonlocal model. The governing equations in differential form together with associated constitutive boundary conditions were then derived. The proposed formulation can be used for arbitrary kernel functions. The GDQ technique was also employed to solve the nonlinear bending problem. Selected numerical results were given for geometrically nonlinear bending of FG Timoshenko nanobeams under various end supports. It was shown that the paradox related to clamped–free boundary conditions is resolved by the present approach. Moreover, the effects of nonlocal parameter, FG index, length-to-thickness ratio and nonlinearity were illustrated.

## References

1. Gurtin, M.E., Murdoch, A.I.: A continuum theory of elastic material surface. *Arch. Ration. Mech. Anal.* **57**, 291–323 (1975)
2. Gurtin, M.E., Murdoch, A.I.: Surface stress in solids. *Int. J. Solids Struct.* **14**, 431–440 (1978)
3. Mindlin, R.D.: Micro-structure in linear elasticity. *Arch. Ration. Mech. Anal.* **16**, 51–78 (1964)
4. Mindlin, R.D., Eshel, N.N.: On first strain-gradient theories in linear elasticity. *Int. J. Solids Struct.* **4**, 109–124 (1968)
5. Mindlin, R.D.: Second gradient of strain and surface-tension in linear elasticity. *Int. J. Solids Struct.* **1**, 417–438 (1965)
6. Lam, D.C., Yang, F., Chong, A., Wang, J., Tong, P.: Experiments and theory in strain gradient elasticity. *J. Mech. Phys. Solids* **51**, 1477–1508 (2003)
7. Eringen, A.C.: Nonlocal polar elastic continua. *Int. J. Eng. Sci.* **10**, 1–16 (1972)
8. Eringen, A.C., Edelen, D.G.B.: On nonlocal elasticity. *Int. J. Eng. Sci.* **10**, 233–248 (1972)
9. Eringen, A.C.: A unified theory of thermomechanical materials. *Int. J. Eng. Sci.* **4**, 179–202 (1966)
10. Eringen, A.C.: Linear theory of nonlocal elasticity and dispersion of plane waves. *Int. J. Eng. Sci.* **10**, 425–435 (1972)
11. Eringen, A.C.: On nonlocal microfluid mechanics. *Int. J. Eng. Sci.* **11**, 291–306 (1973)
12. Eringen, A.C.: Theory of nonlocal electromagnetic elastic solids. *J. Math. Phys.* **14**, 733–740 (1973)
13. Eringen, A.C.: Theory of nonlocal thermoelasticity. *Int. J. Eng. Sci.* **12**, 1063–1077 (1974)
14. Eringen, A.C., Kim, B.S.: Stress concentration at the tip of crack. *Mech. Res. Commun.* **1**, 233–237 (1974)
15. Eringen, A.C.: Theory of nonlocal piezoelectricity. *J. Math. Phys.* **25**, 717–727 (1984)
16. Eringen, A.C.: *Nonlocal Continuum Field Theories*. Springer, New York (2002)
17. Eringen, A.C.: On differential equations of nonlocal elasticity and solutions of screw dislocation and surface waves. *J. Appl. Phys.* **54**, 4703–4710 (1983)
18. Peddieson, J., Buchanan, G.R., McNitt, R.P.: Application of nonlocal continuum models to nanotechnology. *Int. J. Eng. Sci.* **41**, 305–312 (2003)
19. Sudak, L.J.: Column buckling of multiwalled carbon nanotubes using nonlocal continuum mechanics. *J. Appl. Phys.* **94**, 7281–7287 (2003)
20. Wang, Q., Varadan, V.K.: Vibration of carbon nanotubes studied using nonlocal continuum mechanics. *Smart Mater. Struct.* **15**, 659–666 (2006)
21. Rouhi, H., Ansari, R.: Nonlocal analytical Flugge shell model for axial buckling of double-walled carbon nanotubes with different end conditions. *NANO* **7**, 1250018 (2012)
22. Arash, B., Wang, Q.: A review on the application of nonlocal elastic models in modeling of carbon nanotubes and graphenes. *Comput. Mater. Sci.* **51**, 303–313 (2012)
23. Wang, K.F., Wang, B.L., Kitamura, T.: A review on the application of modified continuum models in modeling and simulation of nanostructures. *Acta Mech. Sin.* **32**, 83–100 (2016)
24. Zhang, D., Lei, Y., Shen, Z.: Effect of longitudinal magnetic field on vibration response of double-walled carbon nanotubes embedded in viscoelastic medium. *Acta Mech. Solida Sin.* **31**, 187–206 (2018)
25. Eltahir, M.A., Khater, M.E., Emam, S.A.: A review on nonlocal elastic models for bending, buckling, vibrations, and wave propagation of nanoscale beams. *Appl. Math. Model.* **40**, 4109–4128 (2016)
26. Ansari, R., Rouhi, H., Sahmani, S.: Calibration of the analytical nonlocal shell model for vibrations of double-walled carbon nanotubes with arbitrary boundary conditions using molecular dynamics. *Int. J. Mech. Sci.* **53**, 786–792 (2011)
27. Shen, H.S., Xu, Y.M., Zhang, C.L.: Prediction of nonlinear vibration of bilayer graphene sheets in thermal environments via molecular dynamics simulations and nonlocal elasticity. *Comput. Meth. Appl. Mech. Eng.* **267**, 458–470 (2013)
28. Liang, Y., Han, Q.: Prediction of the nonlocal scaling parameter for graphene sheet. *Eur. J. Mech. A Solids* **45**, 153–160 (2014)
29. Ansari, R., Shahabodini, A., Rouhi, H.: A nonlocal plate model incorporating interatomic potentials for vibrations of graphene with arbitrary edge conditions. *Curr. Appl. Phys.* **15**, 1062–1069 (2015)
30. Wang, Q.: Wave propagation in carbon nanotubes via nonlocal continuum mechanics. *J. Appl. Phys.* **98**, 124301 (2005)
31. Lu, P., Lee, H.P., Lu, C.: Dynamic properties of flexural beams using a nonlocal elasticity model. *J. Appl. Phys.* **99**, 073510 (2006)
32. Reddy, J.N., Pang, S.D.: Nonlocal continuum theories of beams for the analysis of carbon nanotubes. *J. Appl. Phys.* **103**, 023511 (2008)
33. Wang, Q., Liew, K.M.: Application of nonlocal continuum mechanics to static analysis of micro- and nano-structures. *Phys. Lett. A* **363**, 236–242 (2007)
34. Abazari, A.M., Safavi, S.M., Rezazadeh, G., Villanueva, L.G.: Modelling the size effects on the mechanical properties of micro/nano structures. *Sensors* **15**, 28543–28562 (2015)
35. Challamel, N., Zhang, Z., Wang, C.M., Reddy, J.N., Wang, Q., Michelitsch, T., Collet, B.: On non-conservativeness of Eringen's nonlocal elasticity in beam mechanics: correction from discrete-based approach. *Arch. Appl. Mech.* **84**, 1275–1292 (2014)
36. Khodabakhshi, P., Reddy, J.N.: A unified integro-differential nonlocal model. *Int. J. Eng. Sci.* **95**, 60–75 (2015)
37. Fernández-Sáez, J., Zaera, R., Loya, J.A., Reddy, J.N.: Bending of Euler–Bernoulli beams using Eringen's integral formulation: a paradox resolved. *Int. J. Eng. Sci.* **99**, 107–116 (2016)
38. Zhu, X., Li, L.: Twisting statics of functionally graded nanotubes using Eringen's nonlocal integral model. *Compos. Struct.* **78**, 87–96 (2017)
39. Norouzzadeh, A., Ansari, R.: Finite element analysis of nano-scale Timoshenko beams using the integral model of nonlocal elasticity. *Phys. E* **88**, 194–200 (2017)
40. Norouzzadeh, A., Ansari, R., Rouhi, H.: Pre-buckling responses of Timoshenko nanobeams based on the integral and differential models of nonlocal elasticity: an isogeometric approach. *Appl. Phys. A* **123**, 330 (2017)
41. Tuna, M., Kirca, M.: Exact solution of Eringen's nonlocal integral model for bending of Euler–Bernoulli and Timoshenko beams. *Int. J. Eng. Sci.* **105**, 80–92 (2016)

42. Koutsoumaris, C.C., Eptameris, K.G., Tsamasphyros, G.J.: A different approach to Eringen's nonlocal integral stress model with applications for beams. *Int. J. Solids Struct.* **112**, 222–238 (2017)
43. Romano, G., Barretta, R.: Nonlocal elasticity in nanobeams: the stress-driven integral model. *Int. J. Eng. Sci.* **115**, 14–27 (2017)
44. Romano, G., Barretta, R.: Stress-driven versus strain-driven nonlocal integral model for elastic nano-beams. *Compos. Part B* **114**, 184–188 (2017)
45. Romano, G., Barretta, R., Diaco, M.: On nonlocal integral models for elastic nano-beams. *Int. J. Mech. Sci.* **131–132**, 490–499 (2017)
46. Romano, G., Barretta, R., Diaco, M., Marotti de Sciarra, F.: Constitutive boundary conditions and paradoxes in nonlocal elastic nano-beams. *Int. J. Mech. Sci.* **121**, 151–156 (2017)
47. Romano, G., Luciano, R., Barretta, R., Diaco, M.: Nonlocal integral elasticity in nanostructures, mixtures, boundary effects and limit behaviours. *Contin. Mech. Thermodyn.* **30**, 641–655 (2018)
48. Apuzzo, A., Barretta, R., Luciano, R., Marotti de Sciarra, F., Penna, R.: Free vibrations of Bernoulli–Euler nano-beams by the stress-driven nonlocal integral model. *Compos. Part B Eng.* **123**, 105–111 (2017)
49. Faraji Oskouie, M., Ansari, R., Rouhi, H.: Bending of Euler–Bernoulli nanobeams based on the strain- and stress-driven nonlocal integral models: a numerical approach. *Acta Mech. Sin.* **34**, 871–882 (2018)
50. Faraji Oskouie, M., Ansari, R., Rouhi, H.: A numerical study on the buckling and vibration of nanobeams based on the strain- and stress-driven nonlocal integral models. *Int. J. Comput. Mater. Sci. Eng.* **7**, 1850016 (2018)
51. Faraji Oskouie, M., Ansari, R., Rouhi, H.: Stress-driven nonlocal and strain gradient formulations of Timoshenko nanobeams. *Eur. Phys. J. Plus* **133**, 336 (2018)
52. Faraji Oskouie, M., Norouzzadeh, A., Ansari, R., Rouhi, H.: Bending of small-scale Timoshenko beams based on the integral/differential nonlocal–micropolar elasticity theory: a finite element approach. *Appl. Math. Mech. Eng. Ed.* **40**, 767–782 (2019)
53. Eltaher, M.A., Abdelrahman, A.A., Al-Nabawy, A., Khater, M., Mansour, A.: Vibration of nonlinear graduation of nano-Timoshenko beam considering the neutral axis position. *Appl. Math. Comput.* **235**, 512–529 (2014)
54. Barretta, R., Luciano, R., Marotti-de-Sciarra, F., Ruta, G.: Stress-driven nonlocal integral model for Timoshenko elastic nano-beams. *Eur. J. Mech. A Solids* **72**, 275–286 (2018)
55. Reddy, J.N.: *An Introduction to Nonlinear Finite Element Analysis: With Applications to Heat Transfer, Fluid Mechanics, and Solid Mechanics*. OUP, Oxford (2014)